

NASA TECHNICAL NOTE



NASA TN D-2344

NASA TN D-2344

LOAN COPY: RETI
AFWL (WLIL)
KIRTLAND AFB, NM



FLOW EVALUATION IN AN ARC-HEATED HYPERSONIC WIND TUNNEL

by Roger B. Stewart and John E. Grimaud

Langley Research Center

Langley Station, Hampton, Va.



FLOW EVALUATION IN AN ARC-HEATED
HYPERSONIC WIND TUNNEL

By Roger B. Stewart and John E. Grimaud

Langley Research Center
Langley Station, Hampton, Va.

NATIONAL AERONAUTICS AND SPACE ADMINISTRATION

For sale by the Office of Technical Services, Department of Commerce,
Washington, D.C. 20230 -- Price \$0.75

FLOW EVALUATION IN AN ARC-HEATED

HYPERSONIC WIND TUNNEL*

By Roger B. Stewart and John E. Grimaud
Langley Research Center

SUMMARY

An investigation was conducted to determine the thermodynamic and chemical state of initially dissociated air during expansion in a hypersonic nozzle. Results of tests in conical nozzles having total divergence angles of 10° and 16° indicated an equilibrium expansion for stagnation temperatures on the order of $3,600^\circ\text{K}$ and stagnation pressures of 12 and 20 atmospheres. (A computer program predicted that significant departure from equilibrium would occur at these stagnation conditions.) The method employed for defining the state of the gas was based on independent measurements at corresponding locations of wall static pressures and center-line pitot pressures. Good agreement was found between Mach numbers as determined from measured wall pressures and Mach numbers determined from measured pitot pressures. The measured pressures were used with calculated real-gas flow properties to obtain local values of Reynolds number, effective core size, density, velocity, and the oxygen dissociation fraction.

INTRODUCTION

Reentry simulation in high-enthalpy hypersonic wind tunnels may produce results significantly altered from free-flight conditions because of departures from equilibrium during the nozzle expansion. Also, in an equilibrium expansion, real-gas effects due to chemical reactions can significantly alter predicted flow property values from perfect gas results. Thus, to correlate test results with free-flight conditions, an accurate knowledge of the thermodynamic and chemical state of the flow is necessary in any specific nozzle at each set of stagnation conditions.

The effects of the extremely high pressure and temperature gradients in an expansion complicate an accurate analysis of the gas behavior by introducing coupled nonlinear expressions for predicting the flow property and chemical specie variation throughout the expansion. Considerable work has been done in

*The information presented herein is based in part upon a thesis submitted by Roger B. Stewart in partial fulfillment of the requirements for the degree of Master of Aerospace Engineering, University of Virginia, Charlottesville, Virginia, August 1963.

solving one-dimensional flow equations and chemical kinetic equations for a wide range of temperatures and pressures (refs. 1 to 6), and extensive computer programs exist for calculating the free-stream flow properties in an equilibrium or nonequilibrium expansion (refs. 3 and 7). There is, however, little quantitative experimental evidence known to the authors, except for the work of reference 8, that indicates whether or not a given airflow will duplicate the predicted behavior. The uncertainty in predicting the flow properties is due in part to insufficient knowledge of the dissociation-recombination process that actually occurs. This process involves large energy exchanges and relatively large numbers of collisions and is dependent on the kind and amounts of species present and on reaction rates that are not well established at this time.

The present investigation was undertaken to provide a calibration and flow evaluation in a small arc-heated hypersonic wind tunnel. At the same time, a comparison was sought between predicted flow properties and actual measured values. The departure from equilibrium calculated by the method of reference 7 for the two nozzles investigated herein was not observed, rather, the results indicated an equilibrium expansion.

Measurements of the wall static pressures along both nozzles investigated were made at Mach numbers ranging from about 5 to 7.3. Separate measurements of center-line pitot pressures were made at corresponding locations and, in addition, were carried to a downstream equilibrium Mach number of 8.5. All of these measurements were obtained for stagnation temperatures from about 3,200° K to 3,900° K and stagnation pressures of 12 and 20 atmospheres.

SYMBOLS

A	cross-sectional area of nozzle
C_f	skin-friction coefficient
c_p	frozen specific heat defined in equation (9)
h	molar enthalpy
\bar{h}	mass enthalpy
k_r	recombination rate
M	molecular weight of gas
\dot{m}	gas flow rate
N_{Re}	Reynolds number
N_2	molecular nitrogen
O_2	molecular oxygen

O	atomic oxygen
p	pressure
R	gas constant
r	radius
T	temperature
V	velocity
X	species mole fraction
x	axial center-line distance
β	pressure-gradient parameter in local similarity solution of boundary-layer thickness defined in equation (10)
γ	frozen ratio of specific heats defined in equation (8)
ρ	mass density

Subscripts:

aw	adiabatic wall
b	body coordinate
c	cold
f	point of freezing
h	hot
i	chemical species
o	standard reference conditions
t	stagnation conditions
w	wall
x	axial center-line distance
1	free stream
2	behind normal shock

Superscripts:

- ' quantities evaluated at reference condition
- * sonic throat

APPARATUS AND MODELS

This experiment was conducted in the 900-kilowatt continuous-arc tunnel at the Langley Research Center with air as the test medium. The tunnel employed a rotating direct-current arc with water-cooled copper electrodes and was equipped with a 0.133-inch-diameter, circular, contoured throat, which was water cooled. Reference 9 gives a description of the tunnel. Figure 1 is a photograph of the tunnel with the diffuser and exhaust system omitted. Two solid-copper, conical nozzles were used; one had a 10° total divergence angle, and the other had a 16° total divergence angle. Both nozzles expanded to a geometric area ratio of 508 and were uncooled. Figure 2 is a diagram of the two nozzles showing the location of the pressure orifices. Figure 3 shows the water-cooled pitot pressure probe used. Also shown are typical probe and wall orifice locations in the nozzle. Miniature thermopile gages having a usable pressure range of 0.1 to 10 mm Hg were used for all low-static-pressure measurements (fig. 2). Outputs from these gages were recorded by an 18-channel oscillograph. Transducer pressure gages, rated at 1 psia and higher, were used for measurements of upstream static, pitot, and stagnation-chamber pressures.

TEST PROCEDURE

Exact duplication of stagnation conditions was not possible for two reasons. First, determination of stagnation enthalpy is subject to some uncertainty itself. Second, power regulation of the arc was only within 6 percent.

After initiation of the arc, a period of 5 to 10 seconds was required for the wall static pressures to reach steady-state conditions. The average run time was 40 seconds which allowed better than 30 seconds of steady-state readings.

The nose of the pitot probe was located on the nozzle center line at locations corresponding to the wall pressure orifices. (The assumption of radial source flow in the nozzle is made.) No correction to this placement was made by moving the probe downstream a distance equal to the detachment distance; however, the error introduced by the positioning of the probe tip on the constructed arc lines was of very small magnitude. For each test the complete wall-static-pressure distribution was obtained along with one pitot-pressure reading.

EXPERIMENTAL ACCURACY

Stagnation-Enthalpy Determination

One method of evaluating the stagnation enthalpy is the energy-balance technique. In this method the power losses to the cooling water are subtracted from the input power. A low overall efficiency for net energy addition into the test gas (on the order of 10 percent) severely restricts the accuracy of an energy-balance technique, because small errors in determination of the power losses to the cooling water can cause large percentage errors in the determination of power input to the air. The energy-balance technique was not considered sufficiently reliable for the investigation described herein.

The technique, used for determining the enthalpy in this investigation and for which all the noted temperatures apply, was the commonly designated "sonic-throat" method. The stagnation enthalpy determined by the sonic-throat technique was obtained from the following equation for the static enthalpy at a sonic throat:

$$\bar{h}^* = 0.0312 T_c^{1.25} \left(\frac{P_{t,h} \dot{m}_c}{P_{t,c} \dot{m}_h} \right)^{2.5} \quad (1)$$

where \bar{h}^* is in Btu/lb and T_c is in $^{\circ}\text{R}$. This equation agrees within 6 percent with exact calculations for an equilibrium, isentropic expansion from the stagnation chamber to the throat at the enthalpy levels of this investigation. A recent experimental study with the arc jet exhausting through the throat section into a calorimeter has shown that equation (1) produces values of stagnation temperature within ± 5 percent of the stagnation temperatures determined by the total calorimeter.

Flow Expansion and Uniformity

Because of the magnetic rotation of the arc, the possibility of swirl and nonuniform heating exists. At the present time there are no measurements to indicate the magnitude of these effects; however, it is believed that the strong magnetic field used (12,000 gauss) produces rapid mixing which would tend to minimize uneven heating. A plenum chamber downstream of the arc chamber was used for the purpose of allowing complete mixing of the gas and damping of the swirl from the arc. The low axial flow velocity through the plenum chamber (on the order of 100 ft/sec) provided a relatively long dwell time before expansion through the nozzle.

Pressure Measurements

The pressure traces from the oscillograph recorders could be read to ± 0.00035 psia for the thermopile gages and ± 0.0025 psia for the transducer gages. Accuracies quoted for the thermopile gages are ± 1.5 percent of scale reading in

the linear portion of the calibration curve so that at the highest pressure read, the maximum overall accuracy was ± 1.52 percent of actual pressure, or ± 0.0029 psia. At the lowest pressures read, the maximum overall accuracy was ± 5 percent of actual pressure, or ± 0.0005 psia. Quoted accuracy for the transducer gages is ± 1.5 percent so that at the highest pressures read the maximum accuracy was ± 3.5 percent of actual pressure. All gages used in this experiment were calibrated with a primary standard and the experimental wiring scheme at the test site. Only those gages falling within the manufacturers' quoted accuracy were used.

FLOW PROPERTY CALCULATIONS

High-temperature gas flows can exhibit an inability to redistribute energy among the different active modes in times that are small compared with dwell times in a nozzle. Because of this phenomenon, account must be taken of departures from equilibrium.

For reaction times much shorter than dwell times, the flow maintains an equilibrium composition throughout the expansion and the energy release to the stream from the excited modes keeps pace with the sharp pressure and temperature drop. If the net reaction time for the production and removal of a given species is of the same order as nozzle dwell time, then nonequilibrium effects will dominate the flow process in such a way as to produce measurable differences in the stream properties. In the limit, if the net rate of removal of species that occur at high temperatures falls to zero, the flow is chemically frozen and expands in a manner similar to a perfect gas, that is, with a constant ratio of specific heats.

The previous possibilities set limits on the flow property and chemical specie variations for a given high-temperature expansion. Because of the significant changes in flow properties that can occur under different rates of expansion, calculations were needed of the predicted flow property values for specific nozzles and stagnation conditions. A description of the flow property calculations that were used to check the results of the present experiment is given in the following sections.

Equilibrium Flow

The Langley Research Center has a computing program for the equilibrium expansion of air using the equations given in reference 10 but with corrections to several of the constants. From these calculations, plots were made of the variation of stagnation pressure behind a normal shock with free-stream static pressure, which are the two properties measured in this experiment (ref. 11). The normal-shock properties were obtained by use of the conservation equations of mass, momentum, and energy. Neglect of the chemical specie variation in passing through the shock and to the body was made. For a flow with a stagnation temperature below $4,000^\circ\text{K}$ and a pressure above 10 atmospheres, the stagnation pressure behind a normal shock is nearly independent of the free-stream chemical composition and relaxation effects behind the shock.

Nonequilibrium Flow

The Langley Research Center has a computer program for the nonequilibrium expansion of a three-component model of air (O , O_2 , N_2), which uses the equations of reference 7. This program employs only one reaction, that of the dissociation-recombination of oxygen. Because the fraction of atomic nitrogen is several orders of magnitude below that of oxygen, in the temperature range considered herein, this approach should be valid. However, the question of the reaction rate used, is still an open one. Reference 7 used a rate given by the following:

$$k_r = \frac{7.795 \times 10^{-41}}{T^{1/2}} \quad (2)$$

where k_r has the unit $\frac{\text{ft}^6}{(\text{particles})^2(\text{sec})}$. This rate is a corrected form of that given in reference 12 and is in agreement with the rates given in references 13 and 14, which were obtained with molecular oxygen as the third body. Reference 7 assumed molecular nitrogen to have the same influence on dissociation as does molecular oxygen. A discussion of the influence of reaction rates, which at present vary over a rather wide range (ref. 15), is beyond the scope of this paper. However, a check of the nonequilibrium behavior predicted by reference 7 was made by using the more complete program in reference 3. At a stagnation temperature of 4,000° K and a stagnation pressure of 12 atmospheres, the free-stream properties calculated by both programs were in close agreement. In particular, the stream static pressures at an area ratio of 145 differed by less than 7 percent from each other.

The program of reference 7 requires a nozzle geometry as input in order to start the deviation from equilibrium, as well as, to specify the relationship between the expansion and the nozzle center-line coordinate. The shape of the geometric throat section used in the facility of this investigation was used as input; however, downstream of the throat section the effective core size, obtained from pitot measurements, was used to specify the geometry. It was found later that only very slight differences resulted when the geometric shape of the nozzle was used as input. From the computed free-stream properties of this program, normal-shock properties were calculated by using the fluid flow conservation equations. As previously noted, for the pressure and temperatures of interest herein, the assumption of thermodynamic and chemical equilibrium from immediately behind the shock to the body should still be valid.

Frozen Flow

For dwell times that are small compared with reaction times, a frozen expansion would occur in the nozzle. This expansion would characterize a bounding limit on the behavior of a particular gas and would constitute the widest variation from an equilibrium expansion. The following assumptions were made for calculating the frozen stream properties:

- (1) Full equilibration of the translational and rotational energy modes.
- (2) No energy release from vibrational and dissociative energy modes downstream of the throat minimum.
- (3) Equilibration of all energy modes directly behind the shock.
- (4) Air as a mixture of oxygen and nitrogen with the cold mole fraction of oxygen being 21 percent and the cold mole fraction of nitrogen being 79 percent.
- (5) No nitrogen dissociation.

Values of the mole fractions of O , O_2 , and N_2 were obtained from computed properties at the throat minimum for the particular stagnation conditions of interest. For a constant composition expansion, downstream of the throat minimum, the mole fraction of each species remains constant so that by choosing temperature intervals down the nozzle the following equations, from references 16 and 17, can be solved to give the free-stream properties:

$$\frac{p_1}{p_f} = \left(\frac{T_1}{T_f} \right)^{\frac{\gamma}{\gamma-1}} \quad (3)$$

$$\frac{T_1}{T_f} = \left(\frac{\rho_1}{\rho_f} \right)^{\gamma-1} \quad (4)$$

$$\frac{V_1^2}{RT_0} = \frac{V_f^2}{RT_0} + 2 \left(\frac{\bar{h}_f}{RT_0} - \frac{\bar{h}}{RT_0} \right) \quad (5)$$

$$\frac{\bar{h}}{RT_0} = \frac{1}{RT_0} \sum \frac{X_i h_i}{M_i} = \frac{1}{RT_0} \left(\frac{5}{2} X_O \frac{RT}{M_O} + \frac{7}{2} X_{O_2} \frac{RT}{M_{O_2}} + \frac{7X_{N_2}}{2} \frac{RT}{M_{N_2}} \right) \quad (6)$$

$$\frac{A_1}{A_f} = \left(\frac{T_f}{T_1} \right)^{\frac{1}{\gamma-1}} \left(\frac{V_f}{V_1} \right) \quad (7)$$

$$\gamma = \frac{c_p}{c_p - R} \quad (8)$$

$$c_p = \sum X_i c_{p,i} \quad (9)$$

where $c_{p,i}$ is the specific heat for each species.

Normal-shock properties were calculated by use of the conservation of mass, momentum, and energy as in the previous cases. Figure 4 shows the variation of stagnation pressure behind a normal shock with free-stream static pressure as calculated for the three expansions described and also the perfect gas variation. It should be noted that all deviations from equilibrium involve a one-directional shift in the curves shown in figure 4; that is, any departures from equilibrium in the flow will move the nonequilibrium curve in the direction of the frozen curve.

NOZZLE-BOUNDARY-LAYER CALCULATIONS

Because of the present lack of knowledge concerning boundary-layer growth in a reacting flow, an attempt to predict the development of the effective displacement thickness for comparison with the measured thicknesses was made. The fact that the favorable pressure gradient in the nozzle was only steep through the throat region, plus the fact that the upstream portions of the nozzle were highly cooled, led to use of the method of local similarity for computing the boundary-layer thicknesses. The following general features help to establish how the method was applied: First, the nozzle was assumed similar to a body of revolution with the upstream face taken as the stagnation point. Second, the local boundary-layer profiles were assumed similar and were defined by the pressure-gradient parameter of reference 18:

$$\beta = \frac{2}{v_1^2} \frac{\bar{h}_{t,1}}{\bar{h}_1} \frac{dv_1/dx}{p_1 \left(\frac{r}{r_b}\right)^{2j}} \int_0^x p_1 v_1 \left(\frac{r}{r_b}\right)^{2j} dx \quad (10)$$

where for a body of revolution $j = 1$. The inviscid flow is assumed to commence at the stagnation point of the nozzle face. By knowing the nozzle contour and a given stagnation pressure and enthalpy, the β distributions were obtained. The physical displacement thicknesses were calculated by using the similar solutions parameters of reference 18 and the thickness functions of reference 19.

A second approach for calculating real-gas displacement thicknesses was made by using the momentum integral equation of reference 20. An assumed skin-friction law based on the Blasius flat-plate relationship and modified by the reference enthalpy method is written as:

$$C_F = C_F' \frac{\rho'}{\rho_1} \quad (11)$$

where

$$C_F' = \frac{0.664}{\sqrt{N_{Re,x'}}} \quad (12)$$

and ρ' is determined at Eckert's reference enthalpy:

$$h' = 0.5h_w + 0.22h_{aw} + 0.28h_l \quad (13)$$

The computer program of reference 20 was formulated and displacement thicknesses were calculated for an initial potential flow defined by the 10° and 16° total divergence angles.

RESULTS AND DISCUSSION

The use of wall static pressure to determine free-stream static pressure involved several important considerations: First, the expanding flow was assumed to propagate from a source. This is not strictly true, of course, but for the nozzle geometry used, deviation from a one-dimensional flow should not be a critical factor. Second, the Reynolds numbers in both nozzles were sufficiently high (5×10^4 per foot) that the pressure gradient and subsequent pressure change through the boundary layer should be negligible. Finally, a check must be made to verify that downstream pressure disturbances are not fed upstream through the boundary layer along the nozzle wall. In a hypersonic nozzle, large wall pressure increases and subsequent separation can occur as a result of such feedback. Three techniques were used to check for possible disturbances on the wall. In the first technique high pressure was imposed on the nozzle wall by means of shock impingement from the pitot probe. The wall pressure profiles obtained in this manner were compared with profiles obtained with the probe removed from the nozzle. The effects were small in the region corresponding to the nose of the probe. Figure 5 shows a series of nozzle wall static pressure profiles with the probe at two different locations in the nozzle (figs. 5(a) and 5(b)) and with the probe removed from the tunnel (fig. 5(c)). The progressive disturbance at the wall as the probe was moved upstream in the nozzle is seen by a comparison of these figures. The disturbances at the wall with the probe located at a geometric area ratio of 195 as shown in figure 5(b) have increased to an unacceptable magnitude. Therefore, pressures at this pitot-probe location were not considered as being within the required accuracy for this investigation.

The second technique employed a modification of the 10° nozzle in which an extension to a 1-foot-diameter test section was made. See figure 5(d) for modified-tunnel geometry. This modification fortunately allowed for a pressure profile along the original nozzle wall to be obtained with a tunnel back pressure that was two orders of magnitude below the level used during the initial tests reported herein. Two pressure profiles are shown in figure 5(d). The pressure profiles are in close agreement and it is apparent that a complete expansion exists in both configurations with no downstream effects on the upstream flow.

The third technique used to check for possible disturbances on the wall was a comparison of measured pitot pressure and calculated free-stream static pressure for an equilibrium expansion from stagnation conditions. Because nonequilibrium effects are unidirectional tending to decrease static pressure from the equilibrium value, any pressure disturbances at the wall would raise the wall pressure above its equilibrium value and thus provide a check on such disturbances. Because of the complete wall pressure profiles obtained for each run,

the possibility that nonequilibrium effects were being compensated for by disturbances propagating upstream was removed.

The static-pressure profile in the 16° nozzle is shown in figure 5(c). At geometric area ratios equal to those in the 10° nozzle, the static pressures are seen to be lower in the 16° nozzle. The slope of the pressure-profile curve is nearly the same for both nozzles which suggests that the shorter wall length in the 16° nozzle and resulting smaller boundary-layer growth are responsible for these lower pressures.

The center-line pitot pressure distribution in the 10° nozzle and the test section are shown in figure 6. The profiles in the upstream portion of the nozzle are seen to be similar for different stagnation pressures when plotted in nondimensional form. In the test section this similarity did not hold at the higher stagnation pressures where the flow expanded from a final Mach number (based on an equilibrium expansion) of 7.3 to 8.5. The cause of this phenomenon was observed visually in the luminous flow by a lengthening of the first half diamond (shock from the cone-cylinder junction) at a stagnation pressure of 20 atmospheres. Because of the narrow range of stagnation temperatures in this investigation as well as the uncertainty with regard to the accuracy of determining stagnation temperatures, a comparison of enthalpy effects on the expansion parameters does not seem justifiable. Nevertheless, the real-gas effects due to the high stagnation temperature level at which these studies were made were appreciable as seen in figure 7. The real-gas equilibrium, nonequilibrium, and frozen calculations of stagnation pressures behind a normal shock and free-stream static pressure shown in figure 7 were obtained from the previously described computer programs and hand calculations. Figure 7 indicates an equilibrium expansion in both nozzles at a stagnation pressure of 12 atmospheres and also in the 10° nozzle at a stagnation pressure of 20 atmospheres. Some of the experimental points do not fall exactly on the theoretical curves, but this is due to the fact that the theoretical curves were plotted on the basis of average stagnation conditions for the total number of runs indicated by the number of experimental points. (Pitot pressure could be measured at only one location during each run.) It should therefore be noted that the experimental error is not of the magnitude implied by figure 7. If each measured point is compared with the theoretical curve obtained from the particular stagnation conditions for that run, the variation from predicted equilibrium values is very small. For instance, the Mach number determined from the real-gas equilibrium calculations (for a given run) by use of measured static pressure varied at most by 3 percent from the Mach number determined by use of measured pitot pressure.

Verification of an equilibrium expansion permits the use of real-gas flow property tabulations in order to find other properties and the effective area ratio. At the higher stagnation pressures, the displacement thickness was less than that at the low stagnation pressures as expected. The effect on the Mach number of thinning the boundary layer was small, however, due primarily to the fact that high Mach number flows are insensitive to variations in expansion ratio. Figures 8 and 9 show the effect of increasing stagnation pressure. Also shown in these figures are calculated area ratios obtained by using the method of local similarity. Although this should be a valid approach in these nozzles, initial disturbances in the plenum chamber and nozzle entrance due to arc

rotation prevent an accurate description of the early flow. At present there are no experimental data on what the magnitude of such effects may be. Although figures 8 and 9 imply a knowledge of the physical displacement thickness, it is not true that this is known. The reason is that the effective throat area is not known and because of the small throat size boundary-layer growth in this region of the nozzle has a large effect on the core size. The method of reference 18 deals primarily with heat transfer. The integral energy equation is satisfied and it might be anticipated that the calculated thicknesses using this method might not give as reliable an indication of displacement effects as a momentum integral approach. The results tend to bear this out. The effective core size from the boundary-layer calculations of reference 20 was used to obtain equilibrium static pressures previously computed. A plot of predicted static pressure against geometric area ratio in the 10° nozzle is shown in figure 10. The predicted values are 40 percent above measured values at the most upstream nozzle location with good agreement occurring in the downstream portion. As pointed out in reference 20 the prediction of boundary-layer growth in the upstream portion of the nozzle should not be expected to be as reliable as near the exit because of neglect of the terms accounting for the effect of axially symmetric flow. In the small nozzle used herein, this appears to be an important factor.

If stagnation temperatures close to those calculated exist, it seems worthwhile to question the apparent lack of agreement between the predicted nonequilibrium behavior and the measured equilibrium expansion. One unfortunate restriction on this investigation was the inability to produce higher stagnation temperatures. At about $3,600^\circ$ K oxygen is just beginning to dissociate and the measurements attempted were critically dependent on having energy absorbed by this process. Departures from equilibrium are more pronounced as the temperature increases, however, for temperatures much below $3,600^\circ$ K the effects of nonequilibrium behavior would not be discernible. A number of the tests were conducted at temperatures calculated to be $3,900^\circ$ K, but many were calculated closer to $3,600^\circ$ K which is very close to a lower limit as far as measurable effects are concerned. A second point to be noted is that the calculated nonequilibrium behavior of reference 7 is dependent on throat configuration. In this investigation, the geometric throat shape was used for the computations. However, viscous and centrifugal effects in the throat region could reduce the effective temperature gradient and thereby reduce the tendency toward nonequilibrium. It is not known how accurately the rate constants for recombination of oxygen describe the actual kinetic process at temperatures below $4,000^\circ$ K. In order to investigate the effect of the recombination rate on the predicted nonequilibrium flow properties, the recombination rate given in equation (2) was increased an order of magnitude and the nonequilibrium program was run. For a stagnation temperature of $3,600^\circ$ K and stagnation pressure of 12 atmospheres the pressures predicted by using the higher recombination rate were only 1.5 percent above the nonequilibrium pressures predicted by using the rate given by equation (2).

CONCLUDING REMARKS

Simultaneous measurements of stream static pressure measured at the wall and center-line pitot pressure were used to check for nonequilibrium effects in the nozzle flow. Three independent methods were used to insure that wall static pressures were an accurate measure of stream static pressures. The measured pressures showed close agreement with values calculated for an equilibrium expansion as compared with values calculated for a nonequilibrium or a frozen expansion. The equilibrium expansion indicated by these measurements occurred for stagnation pressures of 12 and 20 atmospheres and stagnation temperatures up to 3,900° K in the 10° and 16° conical nozzles used in this investigation. Increasing the recombination rate by an order of magnitude had an insignificant effect on bringing the predicted nonequilibrium pressures into agreement with the measured pressures.

A momentum integral approach using real-gas properties and a modified flat-plate skin-friction law predicted laminar real-gas boundary-layer growth reasonably well in the downstream portion of the 10° conical nozzle used in this investigation.

Langley Research Center,
National Aeronautics and Space Administration,
Langley Station, Hampton, Va., March 6, 1964.

REFERENCES

1. Hall, J. Gordon, Eschenroeder, Alan Q., and Marrone, Paul V.: Inviscid Hypersonic Airflows With Coupled Nonequilibrium Processes. Rep. No. AF-1413-A-2 (AFOSR 2072), Cornell Aero. Lab., Inc., May 1962.
2. Hall, J. Gordon, and Russo, Anthony L.: Studies of Chemical Nonequilibrium in Hypersonic Nozzle Flows. Rep. No. AD-1118-A-6 (Contract AF 18(603)-141), Cornell Aero. Lab., Inc., Nov. 1959.
3. Eschenroeder, Alan Q., Boyer, Donald W., and Hall, J. Gordon: Exact Solutions for Nonequilibrium Expansions of Air With Coupled Chemical Reactions. Rep. No. AF-1413-A-1 (AFOSR 622), Cornell Aero. Lab., Inc., May 1961.
4. Bray, K. N. C.: Departure From Dissociation Equilibrium in a Hypersonic Nozzle. A.R.C. 19,983 (British), Mar. 17, 1958.
5. Boyer, D. W., Eschenroeder, Alan Q., and Russo, A. L.: Approximate Solutions for Nonequilibrium Airflow in Hypersonic Nozzles. Rep. No. AD-1345-W-3 (AEDC TN-60-181), Cornell Aero. Lab., Inc., Aug. 1960.
6. Emanuel, George, and Vincenti, Walter G.: Method for Calculation of the One-Dimensional Nonequilibrium Flow of a General Gas Mixture Through a Hypersonic Nozzle. AEDC-TDR-62-131 (Contract No. AF 40(600)-930), Arnold Eng. Dev. Center, June 1962.
7. Glowacki, Walter J.: Effect of Finite Oxygen Recombination Rate on the Flow Conditions in Hypersonic Nozzles. NOLTR 61-23, U.S. Naval Ord. Lab. (White Oak, Md.), Sept. 15, 1961.
8. Nagamatsu, H. T., Workman, J. B., and Sheer, R. E., Jr.: Hypersonic Nozzle Expansion of Air With Atom Recombination Present. Jour. Aerospace Sci., vol. 28, no. 11, Nov. 1961, pp. 833-837.
9. Boatright, William B., Stewart, Roger B., and Grimaud, John E.: Description and Preliminary Calibration Test of a Small Arc-Heated Hypersonic Wind Tunnel. NASA TN D-1377, 1962.
10. Grabau, Martin: A Method of Forming Continuous Empirical Equations for the Thermodynamic Properties of Air From Ambient Temperatures to 15,000° K, With Applications. AEDC-TN-59-102 (Contract No. AF 40(600)-800), Arnold Eng. Dev. Center, Aug. 1959.
11. Hayman, Lovick O., Jr., and Stewart, Roger B.: A Technique for Determining the Nozzle-Flow Properties of Air in an Equilibrium, Nonequilibrium, or Frozen State. Jour. Aerospace Sci. (Readers' Forum), vol. 29, no. 2, Feb. 1962, p. 245.
12. Heims, Steve P.: Effect of Oxygen Recombination on One-Dimensional Flow at High Mach Numbers. NACA TN 4144, 1958.

13. Byron, Stanley R.: Measurement of the Rate of Dissociation of Oxygen. Jour. Chem. Phys., vol. 30, no. 6, June 1959, pp. 1380-1392.
14. Matthews, D. L.: Interferometric Measurement in the Shock Tube of the Dissociation Rate of Oxygen. The Physics of Fluids, vol. 2, no. 2, Mar.-Apr. 1959, pp. 170-178.
15. Anderson, Thomas P.: The Effect of Recombination Rate on the Flow of a Dissociating Diatomic Gas. AEDC-TR-61-12 (Contract No. AF 40(600)-748), Arnold Eng. Dev. Center, Sept. 1961.
16. Heims, Steve P.: Effects of Chemical Dissociation and Molecular Vibrations on Steady One-Dimensional Flow. NASA TN D-87, 1959.
17. Penner, S. S.: Chemistry Problems in Jet Propulsion. Pergamon Press, 1957.
18. Beckwith, Ivan E., and Cohen, Nathaniel B.: Application of Similar Solutions to Calculation of Laminar Heat Transfer on Bodies With Yaw and Large Pressure Gradient in High-Speed Flow. NASA TN D-625, 1961.
19. Cohen, Nathaniel B.: Boundary-Layer Similar Solutions and Correlation Equations for Laminar Heat-Transfer Distribution in Equilibrium Air at Velocities up to 41,100 Feet Per Second. NASA TR R-118, 1961.
20. Durand, J. A., and Potter, J. Leith: Calculation of Thicknesses of Laminar Boundary Layers in Axisymmetric Nozzles With Low-Density, Hypervelocity Flows. AEDC-TN-61-146 (Contract No. AF 40(600)-800 S/A 24(61-73)), Arnold Eng. Dev. Center, Dec. 1961.

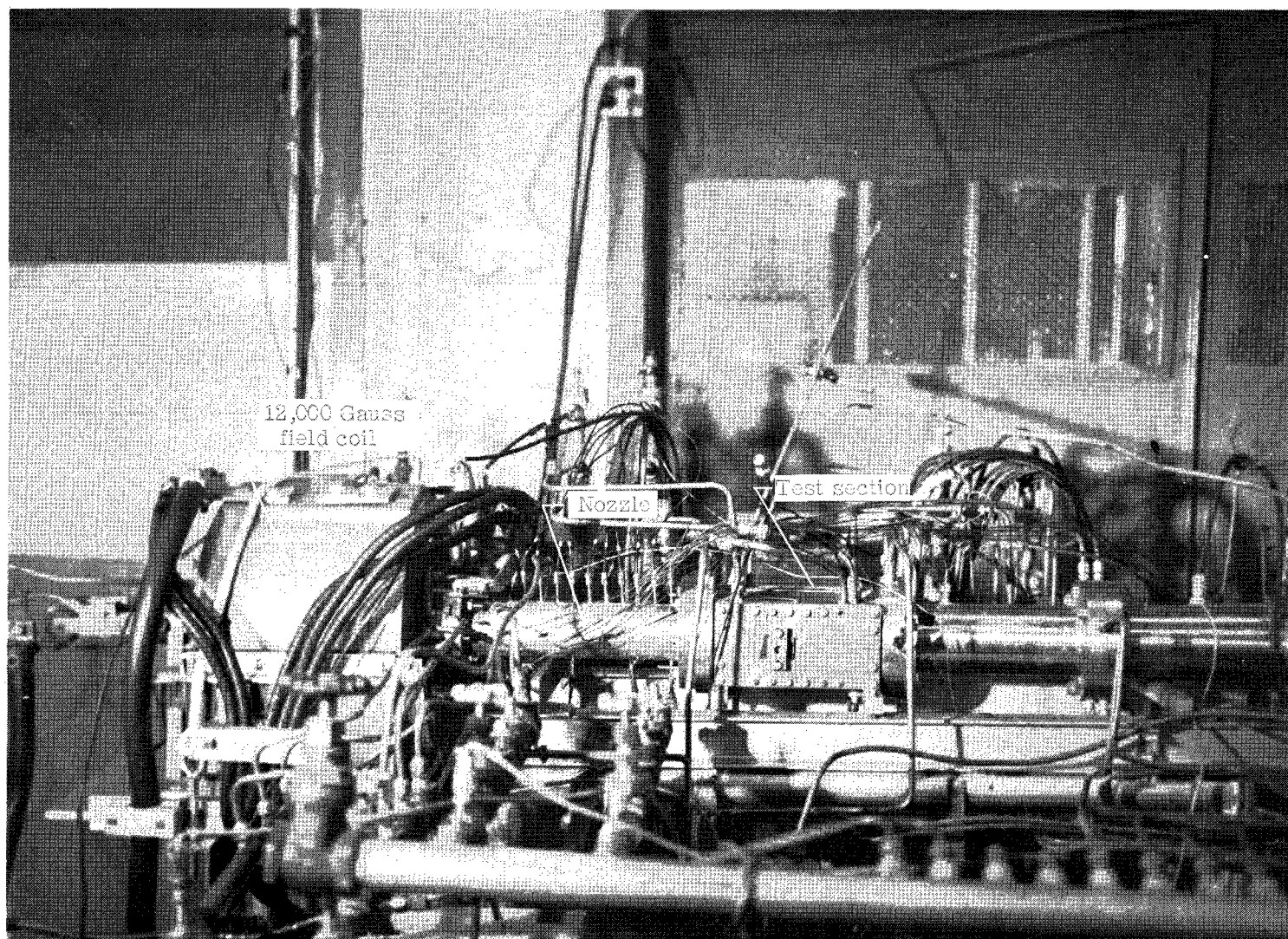
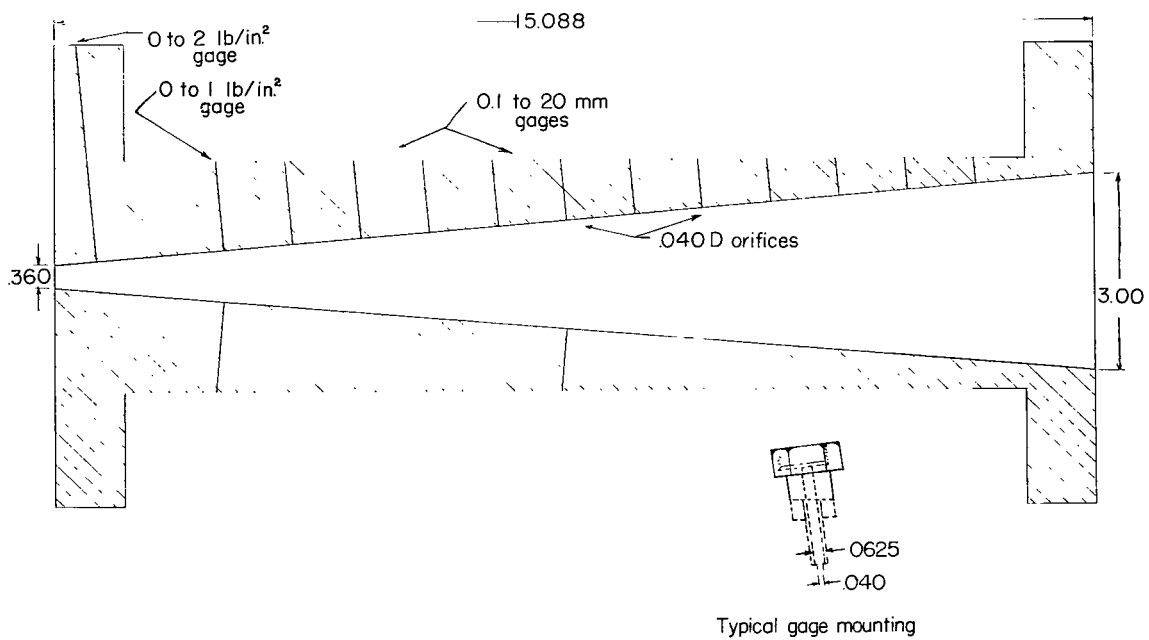
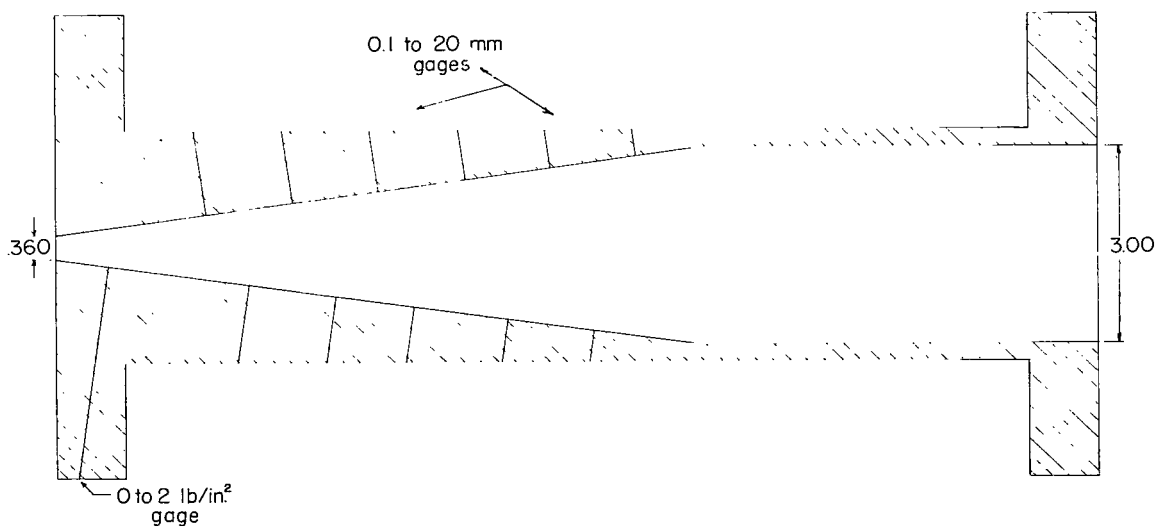


Figure 1.- The 900-kilowatt continuous-arc tunnel.

L-64-3015



(a) 10° conical nozzle.



(b) 16° conical nozzle.

Figure 2.- Static-pressure orifice locations for 10° and 16° nozzles.

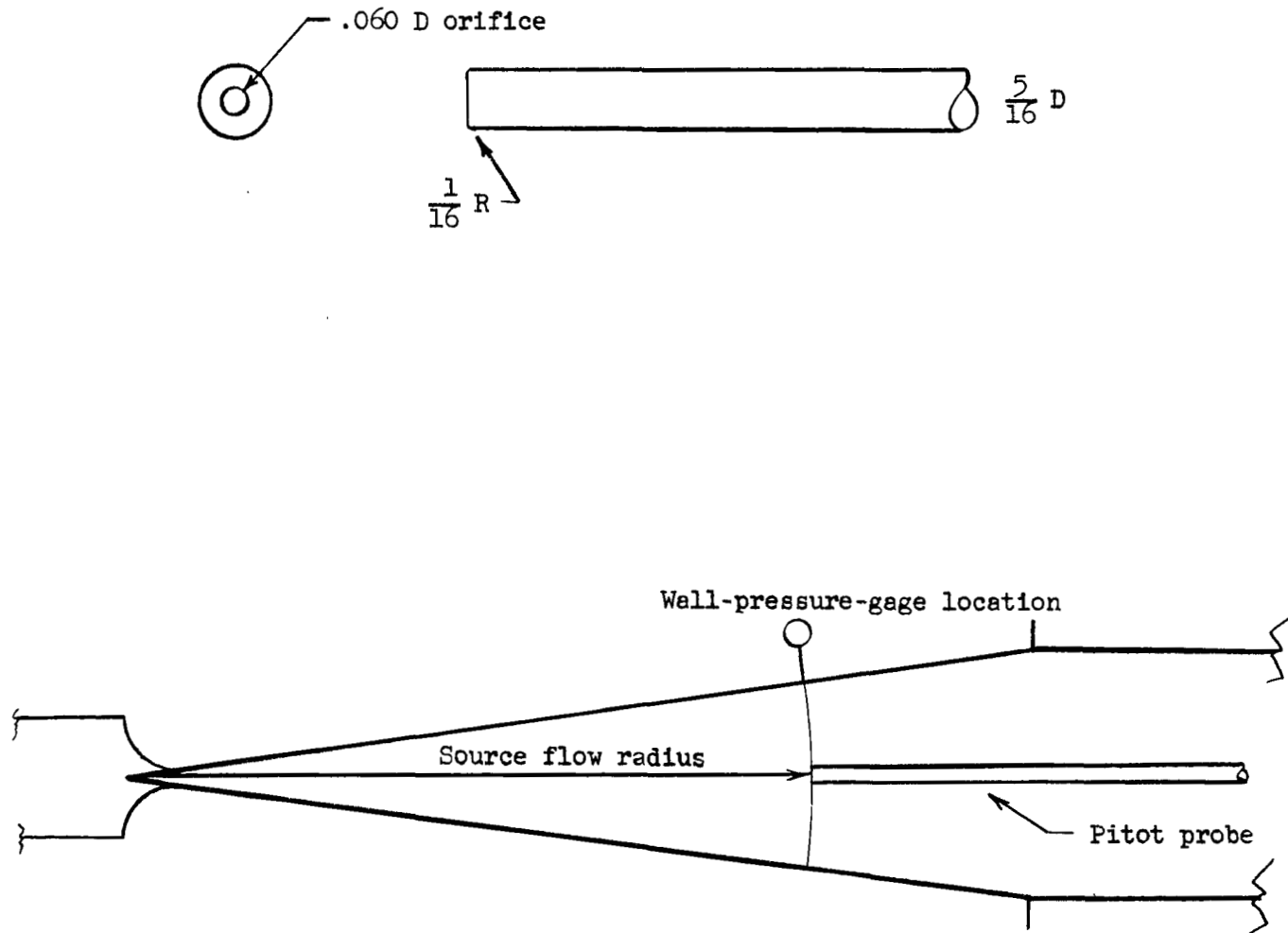


Figure 3.- Pitot probe and typical location in nozzle.

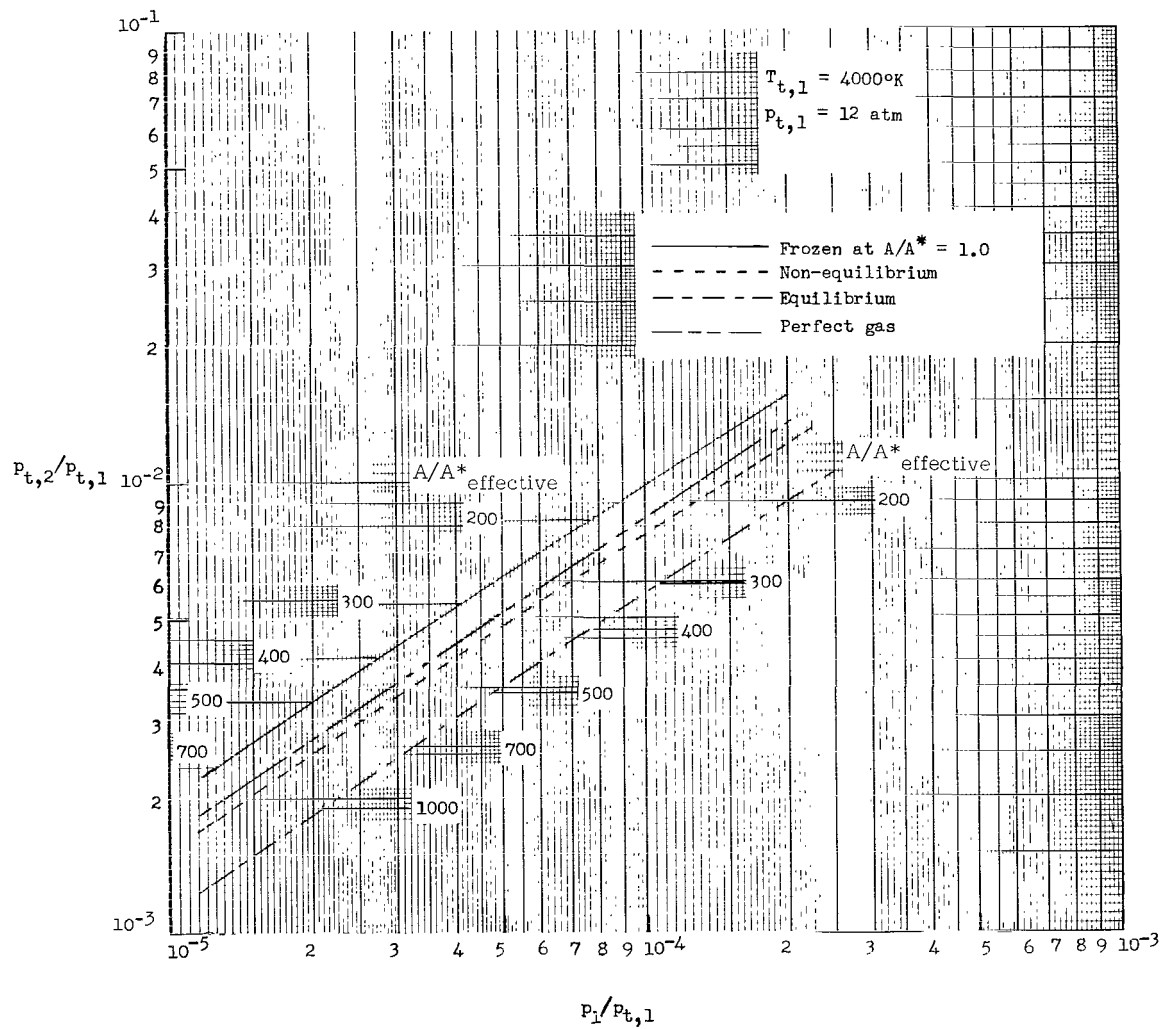
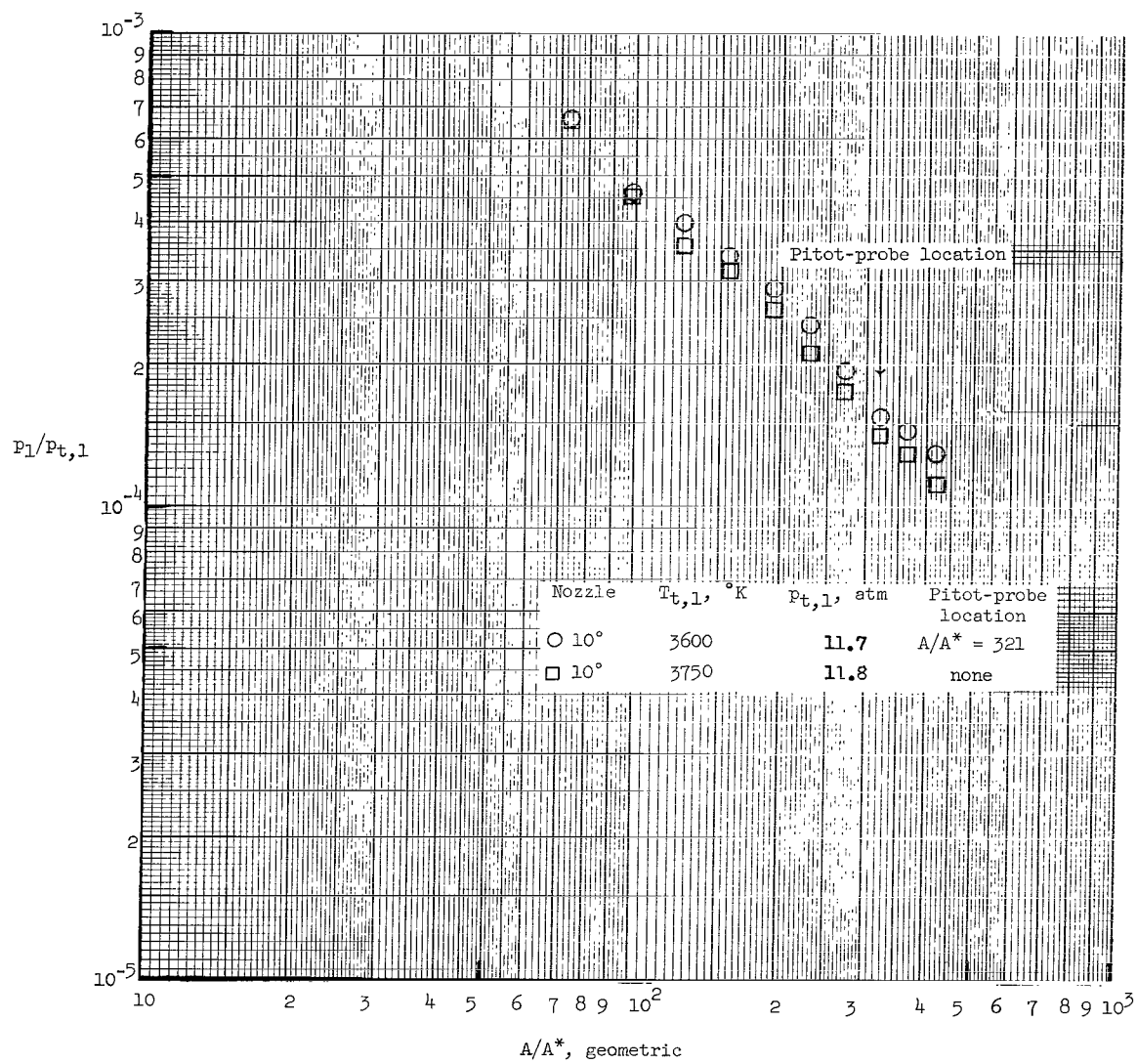
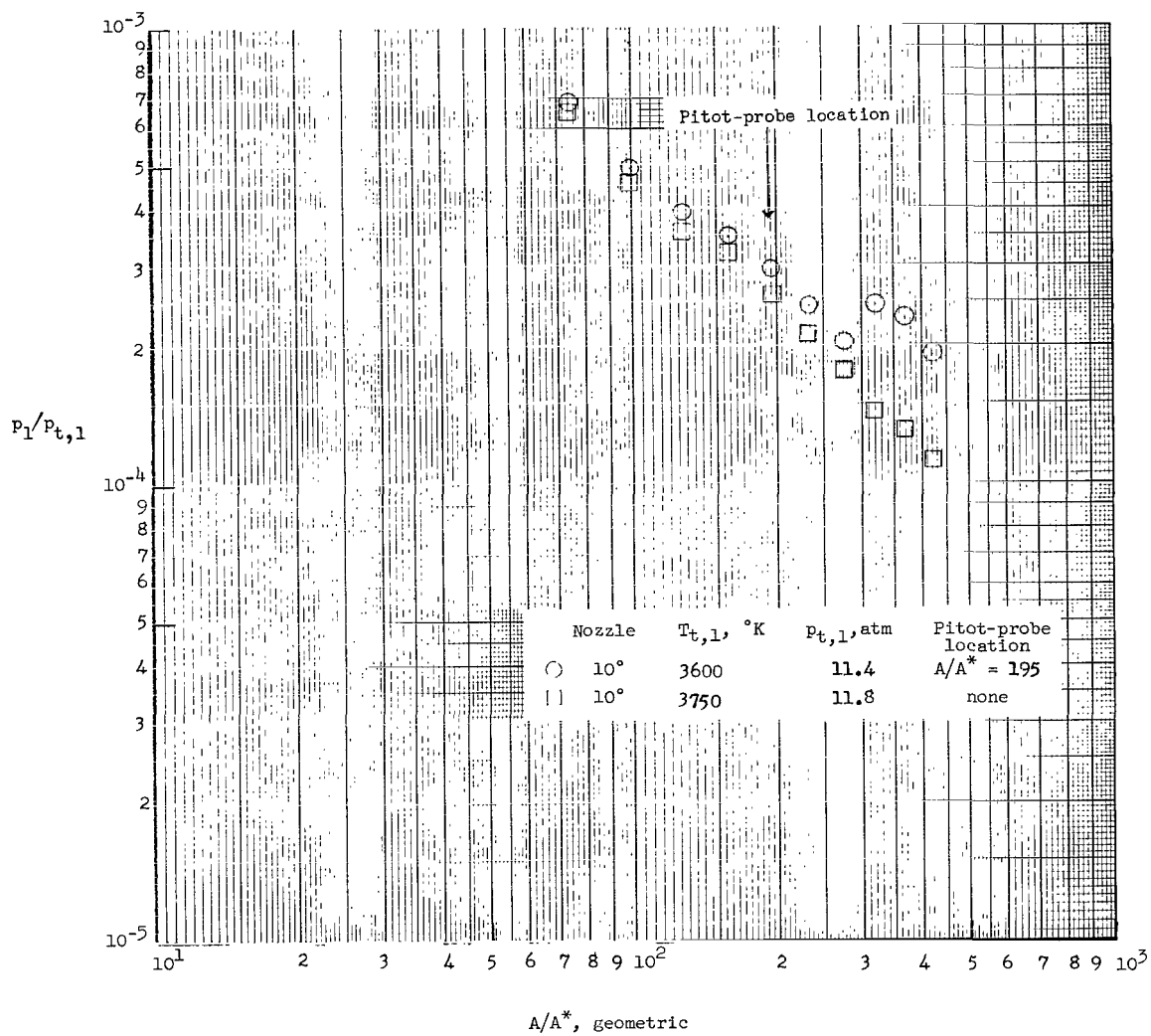


Figure 4.- Variation of stagnation pressure behind a normal shock with stream static pressure.



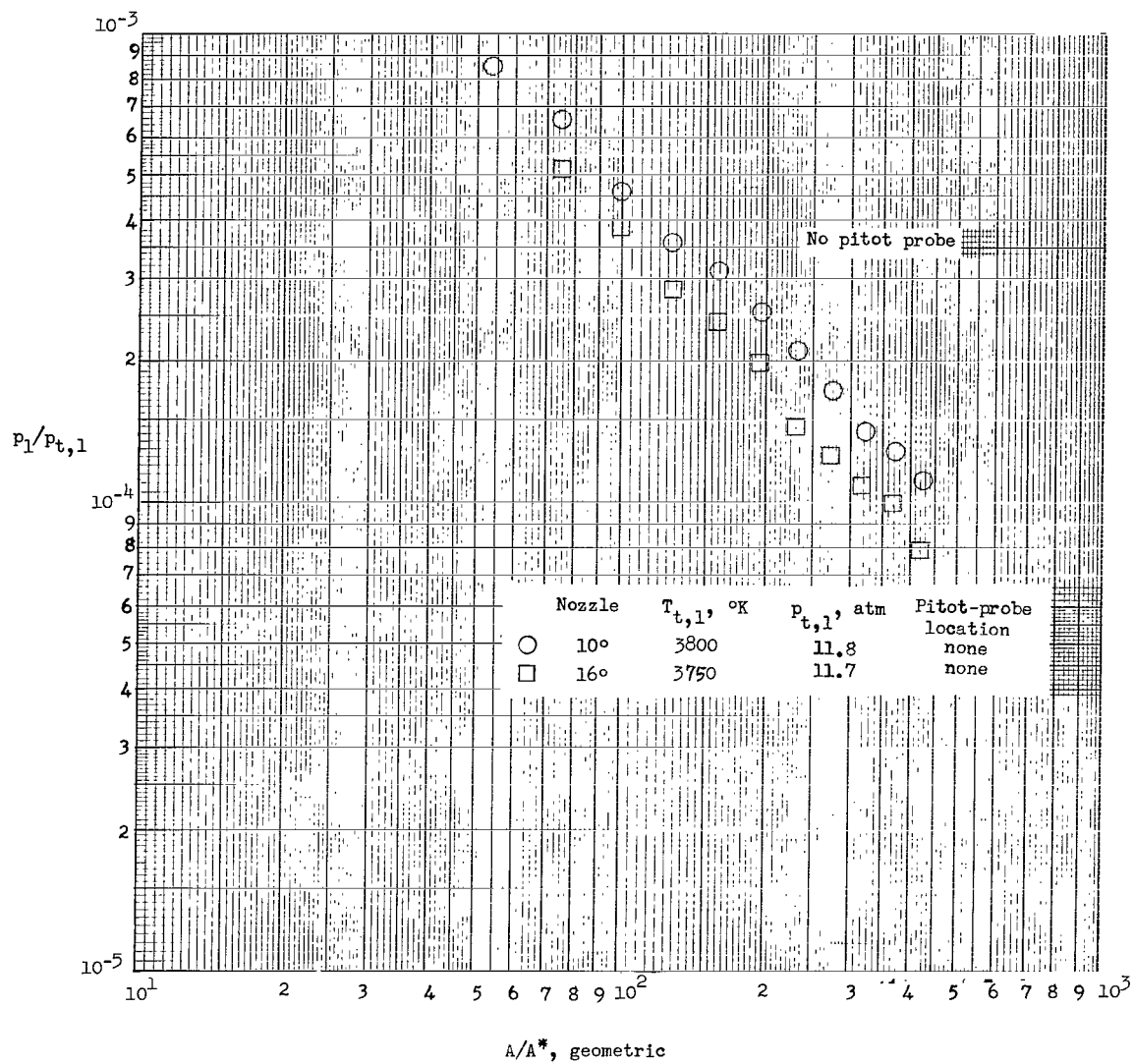
(a) Probe effect.

Figure 5.- Measured wall static pressure.



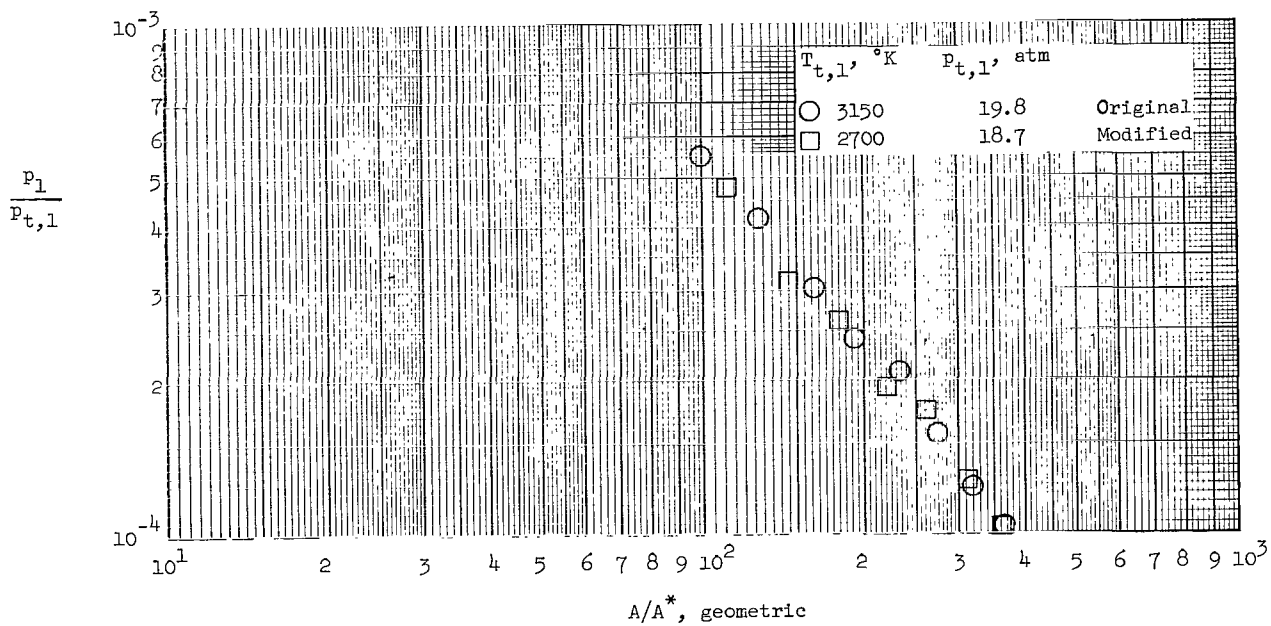
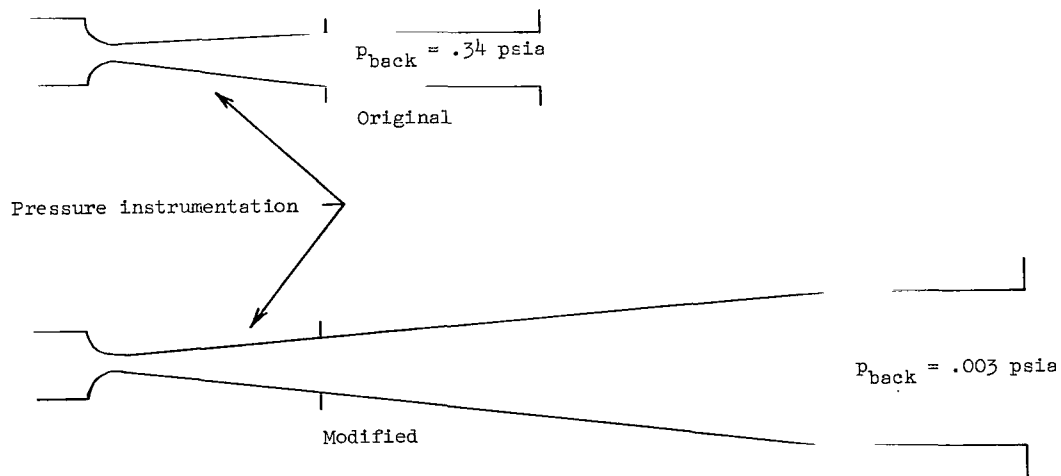
(b) Upstream probe location.

Figure 5.- Continued.



(c) 10° and 16° nozzles.

Figure 5.- Continued.



(d) Pressure profiles for different tunnel back pressures.

Figure 5.- Concluded.

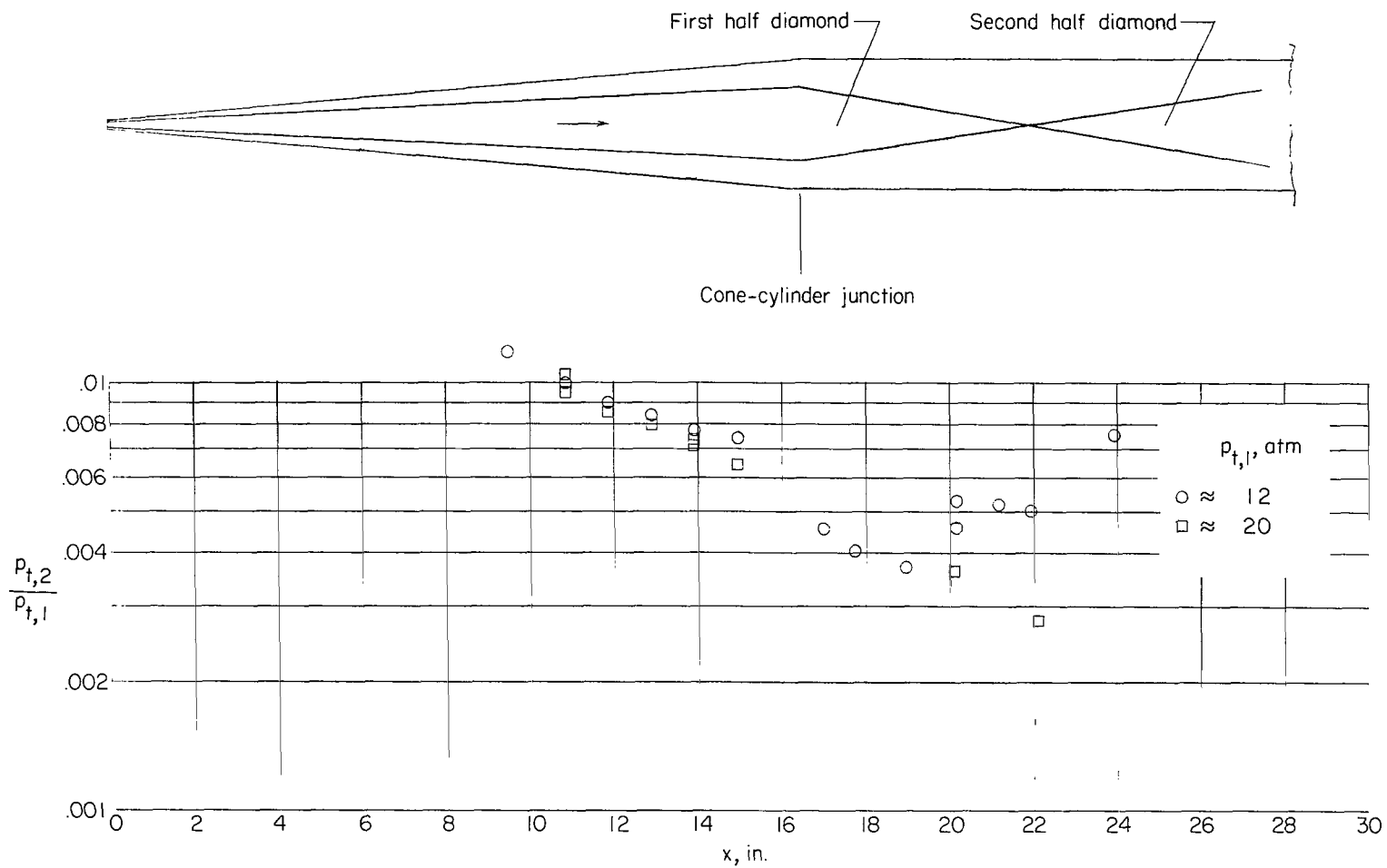
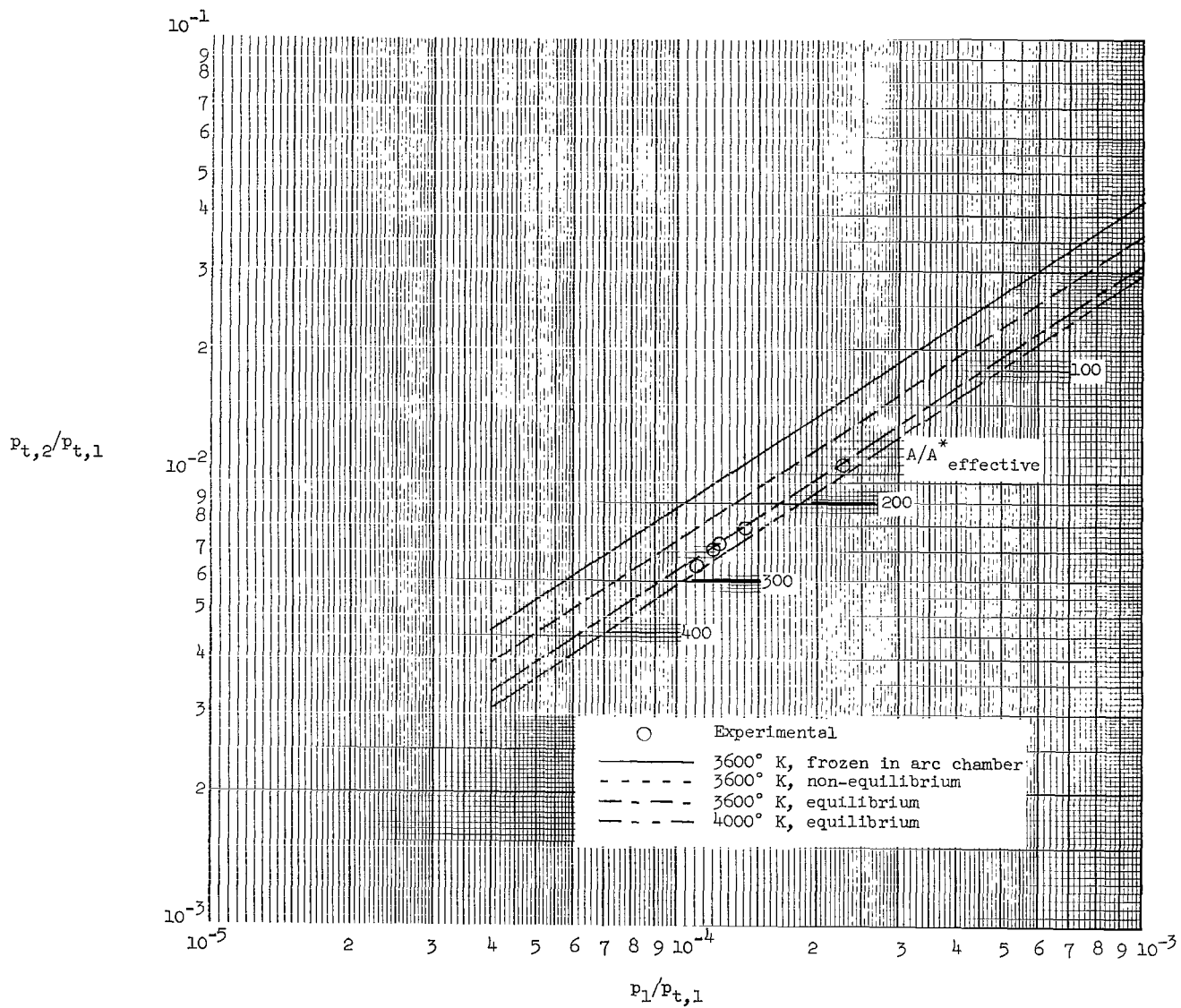
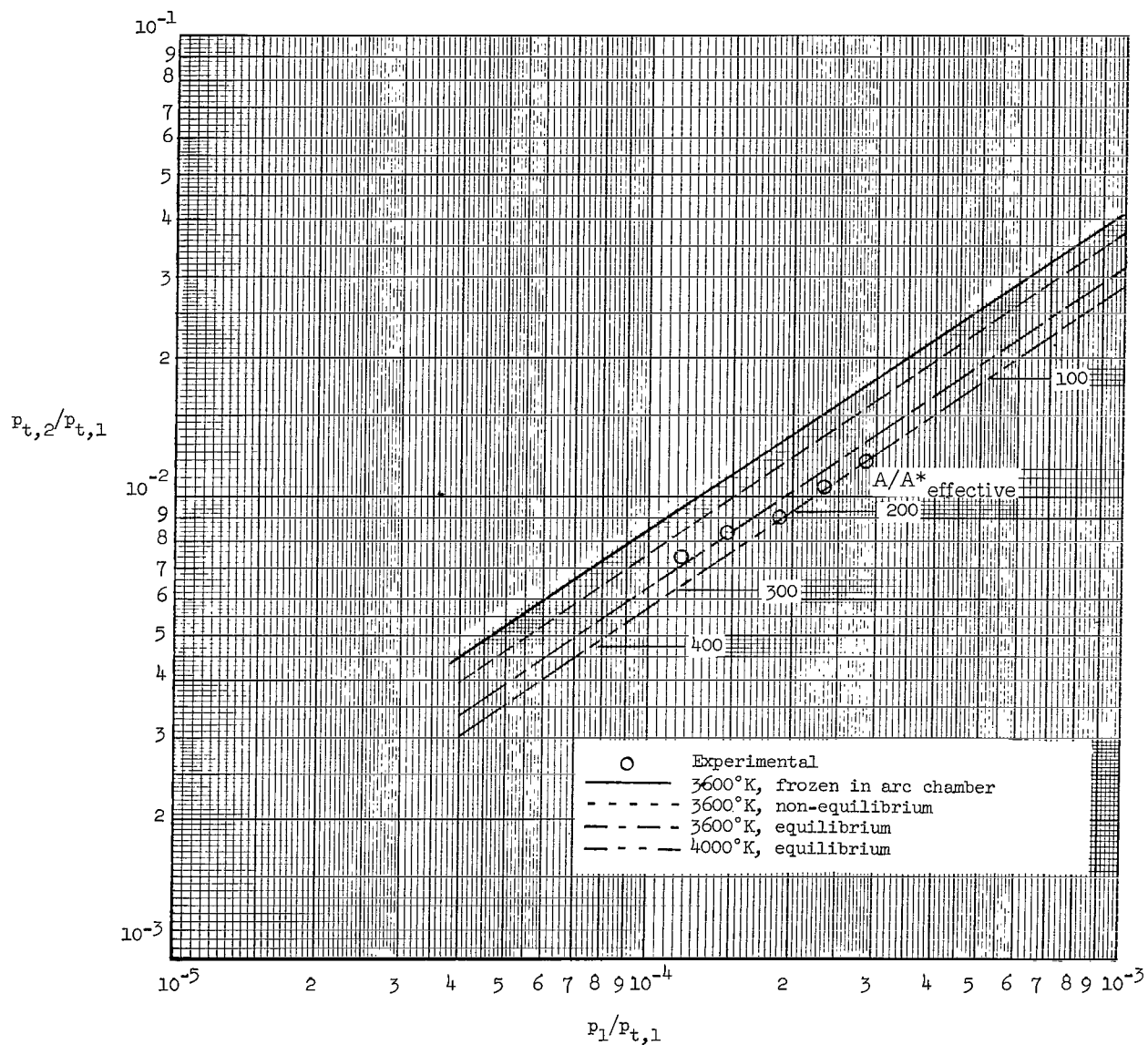


Figure 6.- Longitudinal pitot pressure distribution in 10° nozzle.



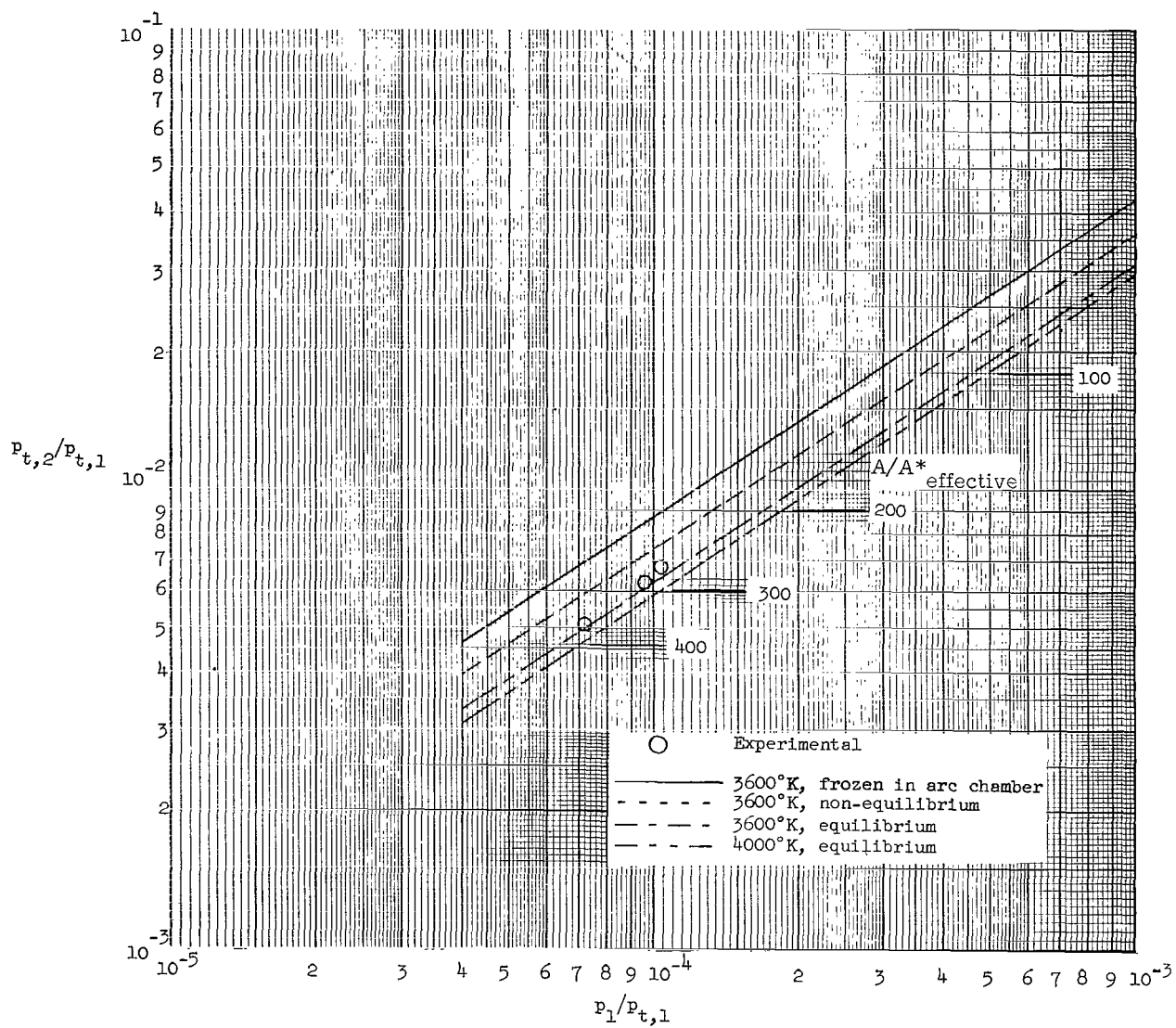
(a) 10° nozzle, $P_{t,1} = 11.6$ atm (average).

Figure 7.- Variation of measured pitot pressure with measured wall static pressure.



(b) 10° nozzle, $p_{t,1} = 20.6$ atm (average).

Figure 7.- Continued.



(c) 16° nozzle, $p_{t,1} = 11.8$ atm (average).

Figure 7.- Concluded.

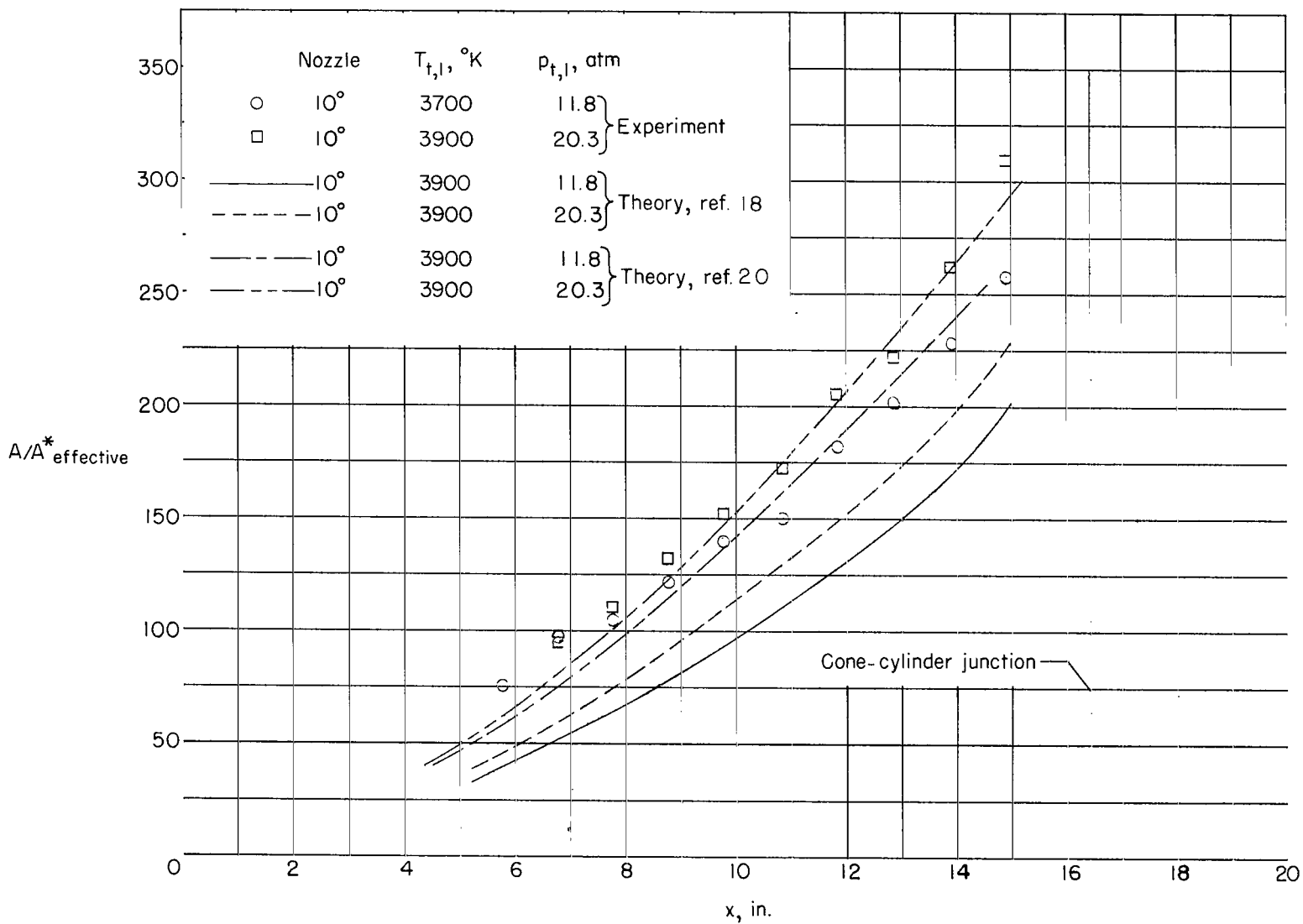


Figure 8.- Variation of boundary-layer thickness with longitudinal center-line distance from throat.

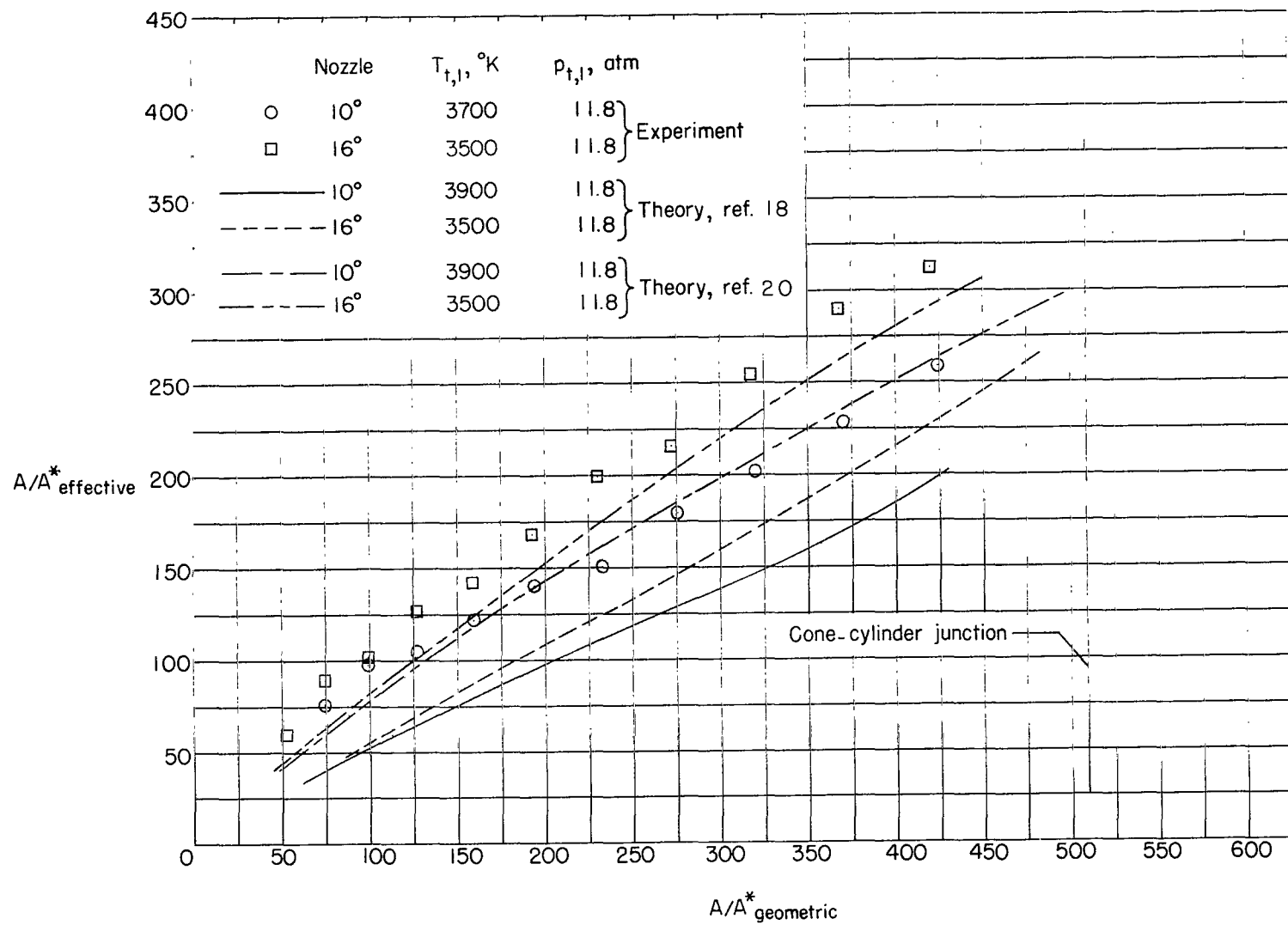


Figure 9.- Effect of nozzle expansion rate on boundary-layer displacement thickness.

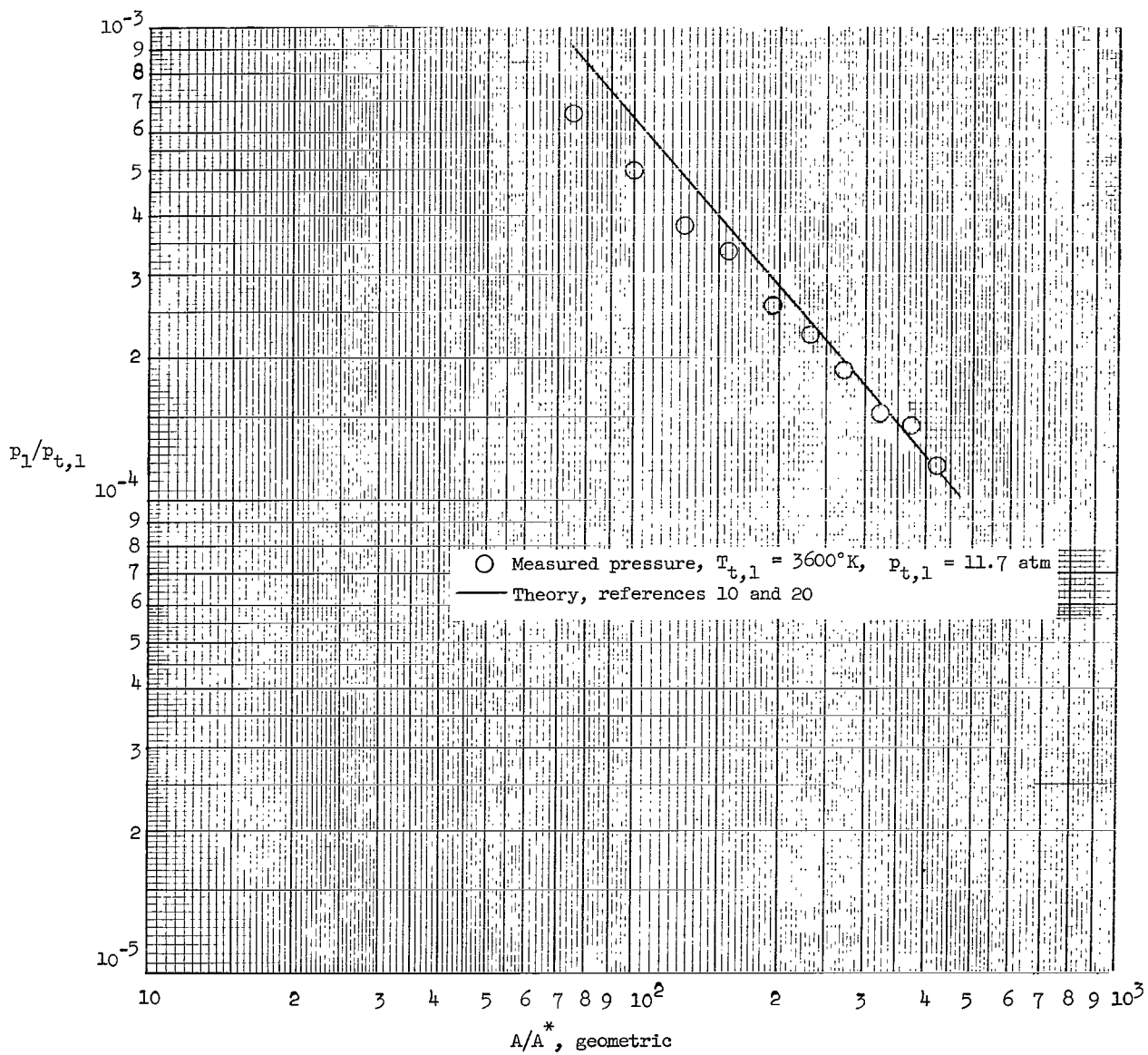


Figure 10.- Comparison of measured and predicted equilibrium static pressure profiles.

2/7/68
G

"The aeronautical and space activities of the United States shall be conducted so as to contribute . . . to the expansion of human knowledge of phenomena in the atmosphere and space. The Administration shall provide for the widest practicable and appropriate dissemination of information concerning its activities and the results thereof."

—NATIONAL AERONAUTICS AND SPACE ACT OF 1958

NASA SCIENTIFIC AND TECHNICAL PUBLICATIONS

TECHNICAL REPORTS: Scientific and technical information considered important, complete, and a lasting contribution to existing knowledge.

TECHNICAL NOTES: Information less broad in scope but nevertheless of importance as a contribution to existing knowledge.

TECHNICAL MEMORANDUMS: Information receiving limited distribution because of preliminary data, security classification, or other reasons.

CONTRACTOR REPORTS: Technical information generated in connection with a NASA contract or grant and released under NASA auspices.

TECHNICAL TRANSLATIONS: Information published in a foreign language considered to merit NASA distribution in English.

TECHNICAL REPRINTS: Information derived from NASA activities and initially published in the form of journal articles.

SPECIAL PUBLICATIONS: Information derived from or of value to NASA activities but not necessarily reporting the results of individual NASA-programmed scientific efforts. Publications include conference proceedings, monographs, data compilations, handbooks, sourcebooks, and special bibliographies.

Details on the availability of these publications may be obtained from:

SCIENTIFIC AND TECHNICAL INFORMATION DIVISION
NATIONAL AERONAUTICS AND SPACE ADMINISTRATION
Washington, D.C. 20546